

First results from the small tight aspect ratio tokamak multifrequency pulse radar reflectometer

V. F. Shevchenko and M. J. Walsh

Citation: *Rev. Sci. Instrum.* **68**, 2040 (1997); doi: 10.1063/1.1148075

View online: <http://dx.doi.org/10.1063/1.1148075>

View Table of Contents: <http://rsi.aip.org/resource/1/RSINAK/v68/i5>

Published by the [American Institute of Physics](#).

Related Articles

Oblique electron-cyclotron-emission radial and phase detector of rotating magnetic islands applied to alignment and modulation of electron-cyclotron-current-drive for neoclassical tearing mode stabilization

Rev. Sci. Instrum. **83**, 103507 (2012)

0.22 THz wideband sheet electron beam traveling wave tube amplifier: Cold test measurements and beam wave interaction analysis

Phys. Plasmas **19**, 093110 (2012)

Measurements of parallel electron velocity distributions using whistler wave absorption

Rev. Sci. Instrum. **83**, 083503 (2012)

HELIOS: A helium line-ratio spectral-monitoring diagnostic used to generate high resolution profiles near the ion cyclotron resonant heating antenna on TEXTOR

Rev. Sci. Instrum. **83**, 10D722 (2012)

Microwave Doppler reflectometer system in LHD

Rev. Sci. Instrum. **83**, 10E322 (2012)

Additional information on *Rev. Sci. Instrum.*

Journal Homepage: <http://rsi.aip.org>

Journal Information: http://rsi.aip.org/about/about_the_journal

Top downloads: http://rsi.aip.org/features/most_downloaded

Information for Authors: <http://rsi.aip.org/authors>

ADVERTISEMENT

ORTEC MAESTRO[®] V7 MCA Software

For over two decades, MAESTRO has set the standard for Windows-based MCA Emulation. MAESTRO Version 7.0 advances further:

- New!** Windows 7 64-Bit Compatibility with Connections Version 8
- New!** List Mode Data Acquisition for Time Correlated Spectrum Events
- New!** Improved Peak fit calculations
- New!** Improved graphics handling for multiple displays
- New!** Open spectrum files directly from Windows Explorer
- New!** Improved performance with Job Functions and display updates

MAESTRO continues to be the world's most popular nuclear MCA software in a broad range of applications!



**Now 64-bit
Windows 7
Compatible!**

www.ortec-online.com

First results from the small tight aspect ratio tokamak multifrequency pulse radar reflectometer

V. F. Shevchenko

TRINITI, Troitsk, Moscow region, 142092, Russia, CIS

M. J. Walsh

UKAEA Fusion, Abingdon, OXON, OX14 3DB, United Kingdom

(Received 22 October 1996; accepted for publication 20 January 1997)

A multifrequency pulse radar reflectometer (PRR) has been designed, commissioned, and is operating successfully on the small tight aspect ratio tokamak (START). The data obtained with this technique allow the study of the density profile evolution during the shot, revealing aspects of the plasma behavior during such events as the internal reconnection. A simple and effective profile-reconstruction algorithm using the stepwise profile approximation permits the monitoring of the plasma density profile immediately after each shot. Cross checks between the START hydrogen cyanide (HCN) interferometer and the line integral density determined by integrating the PRR generated data shows good agreement. © 1997 American Institute of Physics.

[S0034-6748(97)00705-3]

I. INTRODUCTION

A multifrequency pulse radar reflectometer (MPRR) has been designed to measure electron density profiles on the START tokamak.¹ This is, to our knowledge, the first system of its type that is suitable for analyzing tokamak electron density profiles. The principle of the technique is to measure the absolute value of time delay between a pulse launched toward the plasma and its reflection by a plasma cutoff layer.^{2,3} Using measurements based on several frequencies, in this case four, one can deduce the plasma electron density profile. The time delay for each frequency is directly defined by the coordinates of the corresponding cutoff layer and the line integral density up to that point. The number of frequency channels (spatial sampling) employed in the system is typically a compromise between the desired spatial resolution and the hardware complexity, although in principle a frequency swept pulse reflectometer can be built to solve this problem.

II. GENERAL DESCRIPTION OF PULSE RADAR REFLECTOMETRY ON START

The reflectometer is a self-contained instrument that consists of four independent frequency channels operating sequentially in multichannel mode or with a selected channel in single channel mode. A suitable choice of channel frequencies for the START Tokamak was determined to be 19, 33, 47, and 63 GHz.

Each channel includes a stable cw local oscillator, pulsed microwave amplifier, fast *p-i-n* diode modulator, and microwave video detector with low-noise wide-side-band preamplifier (see Fig. 1). The combination of widely differing frequency channels in a single transmitting antenna is achieved using special bandpass filters. The receiving antenna is arranged in a similar manner. The separation of the probe and receive signals is accomplished by using separate antennas. These antennas each have output apertures of $100 \times 50 \text{ mm}^2$ and are designed to probe the plasma with horizontal polarization.

In order to reduce the influence of variations of the reflected pulse amplitude on the accuracy of the measurement, a special temporal locking method is used.⁴ It allows a locking precision of about 50 ps even with pulse amplitude variations of greater than 40 dB. The temporal locking circuit generates standard emitter coupled logic (ECL) signals which are used for time delay measurements with respect to signals controlling the *p-i-n* diode modulators. The time-to-voltage converter is designed on the basis of a newly introduced integrated circuit (Fujitsu MB43669) that provides good temporal resolution with high stability against external disturbance and temperature variations.⁵ The working parameters of the pulse radar reflectometer are as follows: channel frequencies (critical densities $\times 10^{19} \text{ m}^{-3}$): 19 GHz (0.45); 33 GHz (1.35), 47 GHz (2.74), 63 GHz (4.92); peak microwave power (each channel): $>1 \text{ W}$; pulse duration (half-amplitude): 2 ns; rise time of pulse (0.1–0.9 of amplitude): 1 ns; time between measurements: 10 μs (four channels); 2.5 μs (1 channel); maximum tolerable pulse attenuation: 42 dB; time–amplitude converter jitter: 50 ps; output sensitivity: 1 V/ns; maximum output voltage (load 1 M Ω): $\pm 5 \text{ V}$.

The data acquisition can be based on any analog-to-digital converter (ADC) system with a sampling time of 10 μs in the external clock mode. It is important to use external synchronization from the radar system because valid output data only exists for about 2 μs of the 10 μs for each channel.

III. REFLECTOMETER DATA TREATMENT

Even a relatively simple consideration of the pulse radar data can give useful information about plasma density behavior (see Fig. 2). It is easy to find times where the cutoffs appear and disappear for different frequency channels. These time points are indicated by a changing of sign of the measured time delays or more accurately by changing of the sign of the time derivative of the raw radar signals. There are two main processes affecting the measured time delay: the delay due to transparent plasma layers, which should be negative with respect to the vacuum value, and the movement of the

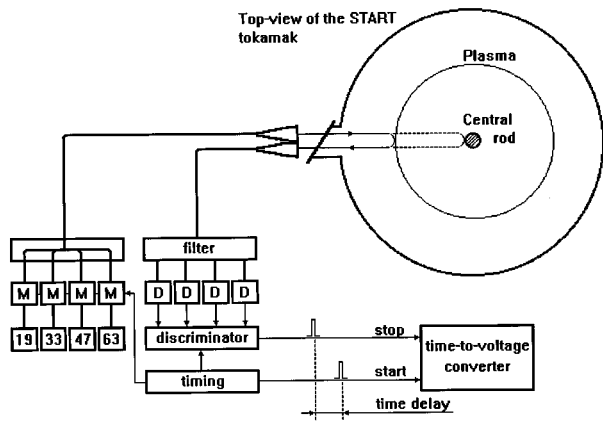


FIG. 1. Block diagram of MPRR on START.

reflecting surface, which always gives a positive contribution in the total time delay. In order to get density profile information an inversion procedure is applied.

PRR allows the measurements of absolute values of

group time delays of microwave pulses reflected from the plasma cutoff layers given by⁶

$$dt(\omega) = \frac{d\varphi(\omega)}{d\omega} = \frac{2}{c} \int_{2a}^{z_{\epsilon=0}} \eta(\omega, z) dz + \frac{2\omega}{c} \int_{2a}^{z_{\epsilon=0}} \frac{d\eta(\omega, z)}{d\omega} dz, \quad (1)$$

where $\varphi(\omega)$ is the phase shift acquired by an electromagnetic wave with gyrofrequency ω reflected from the plasma, $\eta(\omega, z)$ is a refractive index of the plasma, and $z_{\epsilon=0}$ is the coordinate of the reflecting plasma layer [$\epsilon(\omega, z) = 0$] or reflecting surface. This formula can be applied for both o- and x-mode probing waves in accordance with the plasma conditions.

By having four frequency probing one can write four integral equations for any time slice during the plasma shot. Solving these equations it is possible to deduce the edge plasma density profile and full density profile by applying boundary and symmetry conditions. In order

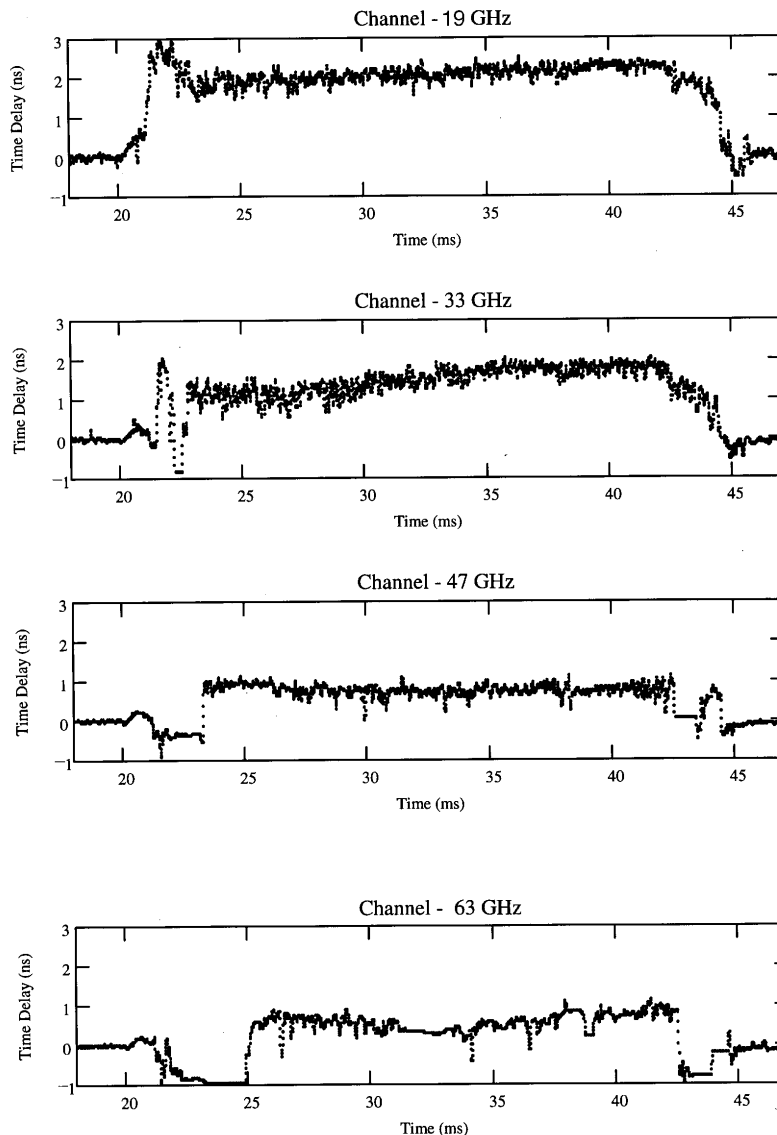


FIG. 2. MPRR signals. The four traces show the response from the MPRR for each of the frequency channels from a typical START plasma (shot no. 23174).

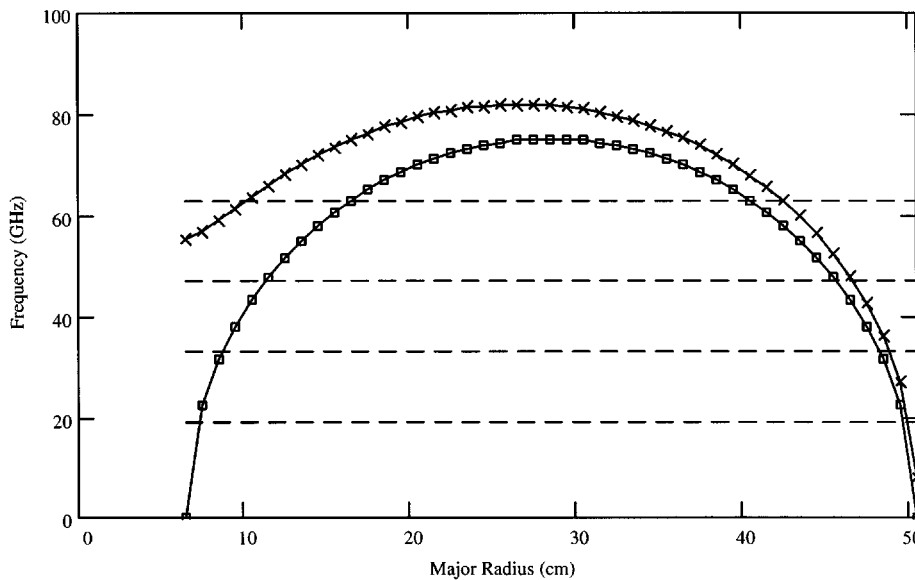


FIG. 3. Location of cutoff layers for parabolic density profile ($N_{\text{center}} = 7 \times 10^{19} \text{ m}^{-3}$) in START for o mode (\square) and x mode (\times).

to elucidate some special features of the pulse radar system and understand its behavior (Fig. 2), some data are analyzed below.

It is very difficult to arrange pure o- to x-mode probing on the START tokamak because the magnetic-field direction on the plasma boundary can vary significantly during the plasma shot and so actually we can have mixed o,x probing. In theory, the radar should receive two echoes with orthogonal polarizations.

In the START case, magnetic fields can be low and the distance between cutoff layers for o and x modes is usually in the range of 1 cm (see Fig. 3). For this reason the plasma birefringence in START can show itself as an interference between o and x mode echoes. In practice it has been found to be reasonable to apply o-mode treatment for data on all channels without significant error.

Equation (1) is written as a one-dimensional approximation. From geometrical optics one can easily estimate the dimensions of the area of the cutoff layer which is able to reflect microwave power back into the antenna aperture,

$$d_{\text{geom}} \cong \frac{Dh}{4[L - (D/2)]}, \quad (2)$$

where h is the antenna aperture, D is the plasma diameter, and L is the distance from antenna to the center of the plasma. It will be limited to $45 \times 90 \text{ mm}^2$ or smaller for most START plasmas. Actually the situation is much more complicated because the radar probes the plasma using coherent waves and some interference effects will take place. Moreover, if one takes into account that the plasma reflecting layer is normally rippled due to density fluctuations it is necessary to suppose that each irradiated point on the cutoff layer is able to reflect power into a solid angle as large as 2π sr. As a result, the receiving antenna will integrate (mix) all waves with different phases

inside the viewing area. In order to clarify the situation we estimate the size of the zeroth-order interference zone using the formula

$$d_0 \cong \left(\frac{\lambda D [L - (D/2)]}{L} \right)^{1/2}, \quad (3)$$

where λ is the wavelength of the probing beam. Supposing a spherical plasma geometry with a diameter of 1.2 m (as in START) it is easy to find the diameter of the zeroth-order interference zone to be about 90 mm for 19 GHz waves and smaller for shorter wavelengths. This size is comparable with the geometrically estimated area for this channel. This means that interference effects can play an important role in the process of reflection from the plasma for the 19 and 33 GHz channels. For higher frequencies the reflecting area is of the order of three interference zones and so these effects should be negligible. In both cases it is reasonable to interpret the data using reflecting sizes estimated geometrically because the probability of receiving the reflected signal from outside this region drops off exponentially. This gives a thickness of the layer taking part in the reflection to be less than 1 cm (assuming spherical surfaces). Since the jitter in the time measurement is of the order of 80 ps (noise in circuits plus noise in the locking circuit), which is equivalent to less than 1 cm, it is quite reasonable to use the one-dimensional consideration for nonturbulent symmetrical plasmas.

Another important fact that can be concluded from the previous consideration is that the amplitude of pulses reflected from the plasma can vary over a wide range even for a quiescent plasma. Variations in the tolerable range will be compounded by the additional jitter of the output radar signal, which is about 80 ps, but variations exceeding this range will give a missing signal or incorrect value of the measured time delay. Both of these events are easily detectable because the first maintains the previous value of the output signal and the second can yield only a larger value of time delay. If we

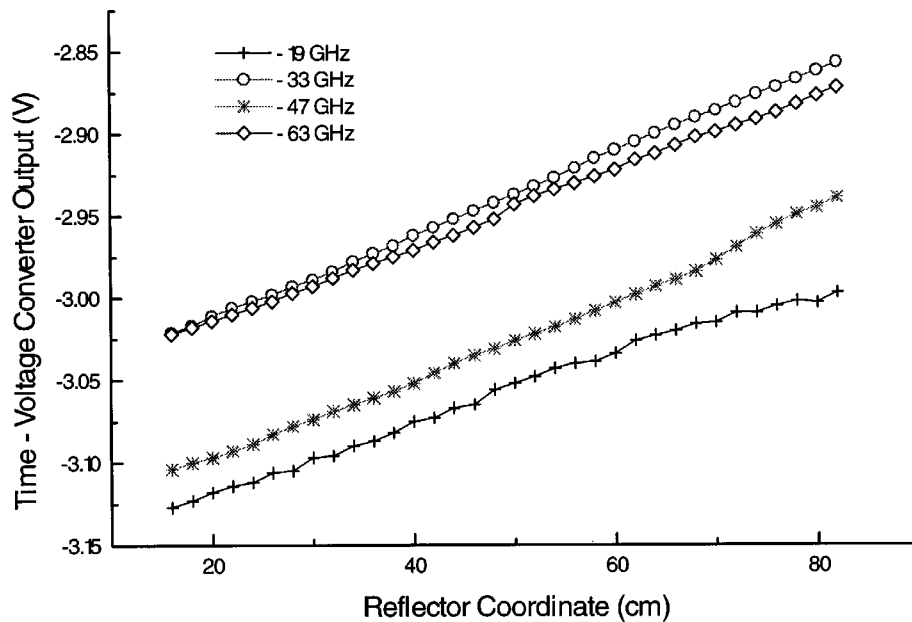


FIG. 4. PRR calibration curves. Note the excellent linearity over the typical operating range of between 20 and 60 cm.

take into account that the plasma is always moving and fluctuating, it would be statistically correct to use a filtering procedure which removes noise (isolated high and low values) and finds the maximum probable value of time delay for any selected time interval of the plasma shot.

IV. CALIBRATION AND ACCURACY OF MEASUREMENTS

In spite of the fact that only one time-to-voltage converter is used for all channels, the output response on the same time delay can be different for different channels because the detectors have characteristics not totally identical and the discriminators can slightly differ. For these reasons it is important to calibrate all channels simultaneously. The calibration scheme is very similar to the experimental scheme but instead the plasma is mimicked by a movable reflector. In this case, the latter was a piece of crushed aluminium foil of $150 \times 200 \text{ mm}^2$ with curvature approximately equivalent to the plasma cutoff surface. The reflector was moved along a rail in steps of 2 cm over a range similar to the START tokamak geometry (approximately 80 cm). Calibration curves are presented in Fig. 4. All channels show good linearity.

The accuracy of the pulse radar measurements can be estimated from the output data jitter. Figure 5 (dotted line) illustrates the typical time delay jitter of the pulse radar output signal while reflections appear only from the central rod (in the absence of plasma). This density function was plotted through 2000 measurements using the second channel of the MPRR. Gaussian fitting to experimental data shows that the jitter of the output signal is typically about 80 ps in real experimental conditions. The application of time-interval filtering through 4–50 measurements increases the accuracy by 2–7 times with a corresponding loss in temporal resolution.

V. FIRST RESULTS AND DENSITY PROFILE RECONSTRUCTION

In order to get initial density profile reconstruction, a simple filtering method was used. This is based on time interval data averaging. The density gradient near the plasma boundary was selected to be fixed for simplicity and its value was estimated from probe measurements in the steady-state regime. This permits the use of radar data only for the rest of the density profile reconstruction. With this assumption the plasma boundary position can be found from the first channel signal,

$$z_0 = \frac{c}{2} (td_1 + \Delta t), \quad (4)$$

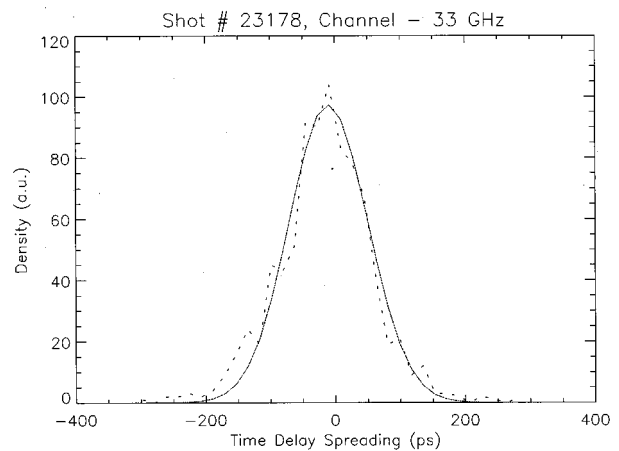


FIG. 5. The typical jitter of the MPRR output signal in plasma absence for the 33 GHz channel. The dotted line represents the experimental data while the solid line represents a Gaussian fit. The typical jitter in the data is about 80 ps. Time-interval filtering can be used to decrease the jitter with a corresponding loss of temporal resolution.

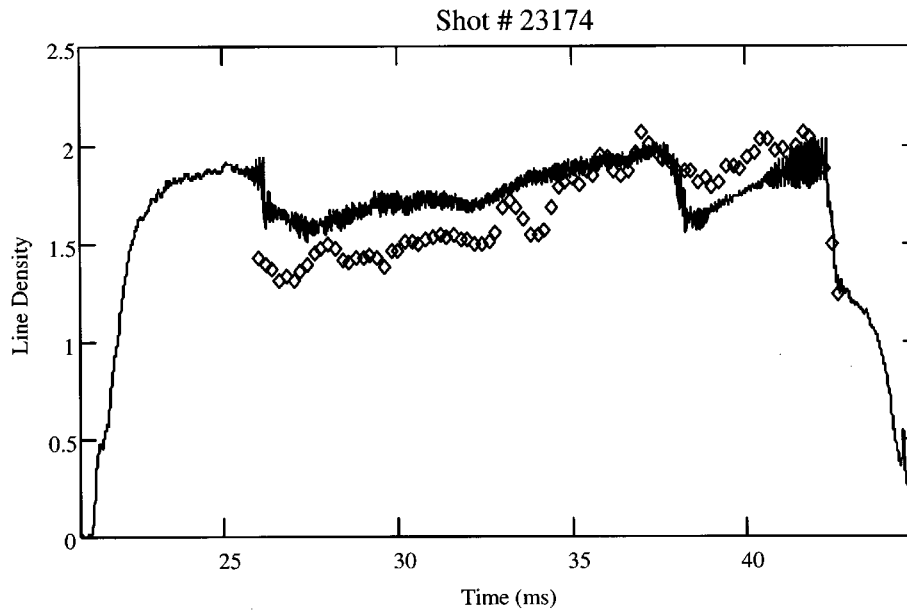


FIG. 6. Comparison of line electron density ($\times 10^{19} \text{ m}^{-2}$) measured by the HCN interferometer and calculated from density profile evolution deduced with the pulse radar data for START shot no. 23174. This figure demonstrates good agreement between the two methods throughout the shot.

where td_1 is the time delay measured by first channel and Δt is a correction due to the outer plasma with gradient ∇n which is estimated from data obtained from the two lowest-frequency channels,

$$\Delta t = \frac{4}{c} \frac{n_1}{\nabla n} \left(1 - \frac{n_0}{n_1} \right)^{1/2}, \quad (5)$$

where n_1 is the plasma cutoff density corresponding to the first channel frequency and n_0 is the edge plasma density. As a first approach one can suppose a piecewise approximation for the density profile. Following this, the coordinates of cutoff layers can be deduced by a simple recurrence formula,

$$z_k = z_{k-1} + \left(\frac{z_0}{2} - \frac{c(td_k)}{4} - \sum_{i=1}^{k-1} \frac{z_i - z_{i-1}}{(1 - (n_{i-1}/n_k))^{1/2} + (1 - (n_i/n_k))^{1/2}} \right) \times \left(1 - \frac{n_{k-1}}{n_k} \right)^{1/2}. \quad (6)$$

Thus we now have five points $(z_0, n_0), (z_1, n_1), \dots, (z_4, n_4)$ from the outer part of the measured plasma density profile. One can suppose, as an approximation, a symmetry of the outer and inner parts of plasma density profile with a corresponding Shafranov shift. Having ten points (four outside, four inside, and two edges) it is possible to plot the whole density profile using any preferred interpolation technique. A parabolic spline interpolation was used for plotting smooth density profiles through the points described above. Changing of the piecewise curve gives an error of about 5% in the definition of cutoff layer positions, so this approach is valid only as a first approximation. It is interesting to compare the reconstructed density profile with independent interferometer data. The line integral plasma density measured by a HCN Michelson interferometer along the central horizontal chord is plotted versus time in Fig. 6. The results obtained by cross integration of density profiles deduced from reflectometer measurements are shown for comparison on the same plot. This figure demonstrates quite good agreement throughout the shot. The difference during the period 29–34 ms implies that the density profile is much more peaked in the central regions of the plasma than is given by a parabolic spline, and flatter than the parabolic spline assumption between 39 and 41 ms, after an internal reconnection has occurred.

Much better agreement between deduced density profiles and experimental data can be achieved using radar and inter-

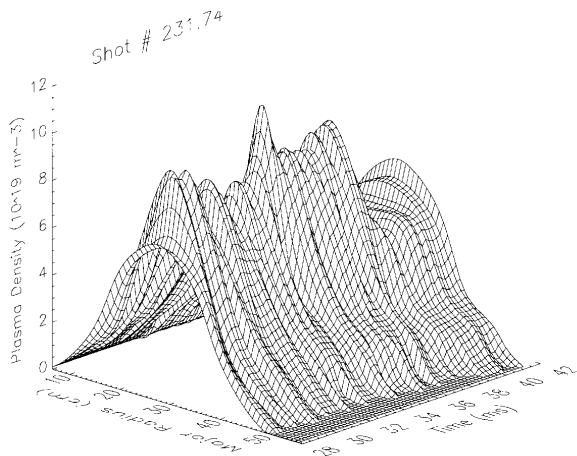


FIG. 7. The plasma density evolution deduced from MPRR and HCN interferometer measurements.

ferometer data together in the reconstruction procedure. Figure 7 illustrates the result of density profile deduction from combined radar and interferometer experimental data. This picture shows the time development of the internal reconnection event in the START tokamak and demonstrates the ability of this diagnostic to follow fast events in the plasma.

ACKNOWLEDGMENTS

This work was funded by the U.K. Department of Trade and Industry and EURATOM. We thank M. Tanaka, National Laboratory for High Energy Physics, Japan, for his help in using the new integrated circuit MB43669 and the

START and COMPASS teams, especially T. Edlington, M. Gryaznevich, I. Jenkins, R. Martin, A. Sykes, and J. Tomas.

¹A. Sykes *et al.*, Nucl. Fusion **32**, 694 (1992).

²V. F. Shevchenko, A. A. Petrov, and V. G. Petrov, Int. J. Infrared Millim. Waves **14**, 1755 (1993).

³C. A. G. Hugengoltz and S. H. Heijnen, Rev. Sci. Instrum. **62**, 1100 (1991).

⁴E. A. Meleshko, *Nanosecond Electronics in Experimental Physics* (Energoatomizdat, Moscow, 1987).

⁵M. Tanaka, H. Ikeda, M. Ikeda, and S. Inaba, Nucl. Instrum. Methods Phys. Res. A **312**, 585 (1992).

⁶V. L. Ginsburg, *Propagation of Electromagnetic Waves in Plasma* (Gordon and Breach, New York, 1961), p. 352.